Proceedings of Engineering and Technology Innovation, vol. 23, 2023, pp. 36-47

Development of a New Ground Motion Model for a Peninsular Indian Rock Site

Ravi Kiran Akella*, Mohan Kumar Agrawal, Jayanta Chattopadhyay

Reactor Safety Division, Bhabha Atomic Research Centre, Mumbai, India

Received 20 July 2022; received in revised form 29 September 2022; accepted 04 October 2022

DOI: https://doi.org/10.46604/peti.2023.10526

Abstract

The ground motion model (GMM) plays a vital role in the generation of seismic design basis ground motion parameters. Even though many intra-plate GMMs are available, very few of them are based on Peninsular India (PI) region-specific seismological parameters. Hence, it is imperative to develop a GMM using seismological parameters derived from earthquakes in the Peninsular Indian region. In this study, a new GMM is developed for a PI rock site. Due to the scarcity of real earthquakes, artificial earthquake records are simulated to generate a new GMM for PI. The accelerograms of these artificial earthquakes are obtained from the stochastic finite fault simulation technique. Region-specific seismological parameters are obtained from the available PI earthquakes. The generated GMM is compared with other intra-plate GMMs for different earthquake magnitudes. Also, the generated GMM is validated with the Koyna earthquake record and it is observed that the GMM's predictions are closer to the record.

Keywords: ground motion model, anelastic attenuation factor, high-frequency decay parameter, stress-drop

1. Introduction

The seismic design of engineering structures requires the evaluation of ground motion parameters during a seismic event such as peak ground acceleration (PGA) or spectral acceleration (SA). The ground motion model (GMM) is a crucial element in seismic hazard assessment to evaluate ground motion parameters due to seismic events. GMM provides ground motion parameters, and PGA or SA are functions of earthquake magnitude and distance. GMM can be developed using regression from actual earthquake records or using artificial earthquakes. Method of regression from actual earthquake records can be used for inter-plate regions, where plenty of real earthquake records are available. For intra-plate regions, seismicity rates are less and hence the method of regression from artificial earthquakes is more suitable for the generation of GMM. Intra-plate regions have relatively less fractured crust than inter-plate regions due to less seismicity rates. Therefore, the seismic ground motion characteristics of intra-plate earthquakes are different from inter-plate earthquakes. Intra-plate earthquakes have less attenuation rate due to less fractured crust.

Seismo-tectonically, India is divided into two broad regions [1]. The first region is a seismo-tectonically active inter-plate region, which includes the Himalayan region, the south Tibet Plateau, Andaman–Sumatra, etc. The second region is Peninsular India (PI), in which seismic activity is relatively less in comparison with the first region. It has been designated as a stable continental region (SCR) and is considered an intra-plate region. Sharma et al. [2] provided GMM based on earthquake data for the Himalayan region, which is an active inter-plate region. Ramkrishnan et al. [3] generated GMM for the north and central Himalayan region using actual earthquake record data. Bajaj and Anbazhagan [4] provided attenuation relations for the active

* Corresponding author. E-mail address: arkiran@barc.gov.in

Tel.: +91-22-25993546

region using limited strong ground motion data. Raghu Kanth and Iyengar [5] and NDMA [6] provided a GMM for PI. Also, intra-plate GMMs generated for eastern North America (ENA) may be applicable for PI due to the similarity in seismo-tectonic features [7].

Atkinson and Boore [8] provided attenuation relations for ENA hard-rock sites in 2011. This is a modification for the earlier ground motion relation by Atkinson and Boore [9]. GMM provided by Toro et al. [10] is derived from stochastic simulation and is valid for central North America and ENA. The hybrid empirical GMM by Pezeshk et al. [11] is also applicable to ENA and termed "PEZA". The GMM provided by Campbell [12] is applicable for hard-rock sites of ENA. This was generated using a hybrid approach of GMM generation for ENA from western North America (WNA) data. Silva et al. [13] provided GMM for ENA using regression analysis of simulations. A list of abbreviations used for all GMMs is given in Table 1.

Table 1 Abbreviations used for GMMs

No.	Ref.	Abbreviation used
1	This study	Present-GMM
2	Kanth and Iyengar [5]	RI-2007
3	NDMA [6]	NDMA-2010
4	Atkinson and Boore [8]	AB-2011
5	Toro et al. [10]	Toro-1997
6	Pezeshk et al. [11]	Peza-2011
7	Campbell [12]	CB-2003
8	Silva et al. [13]	Silva-2002

The major limitation of these GMMs [5-13] is that they are either based on seismological parameters of ENA and WNA or several assumptions in consideration of seismological parameters. Hence, it is imperative to develop a GMM using seismological parameters derived from earthquakes in the Peninsular Indian region.

In India, many nuclear power plants and nuclear facilities are located in the Peninsular Indian region. As very limited earthquake data is available for this intra-plate region, regression from artificial earthquakes is considered to be suitable for the generation of GMM for a PI site. The stochastic finite fault simulation technique is used to generate artificial earthquakes. A seismic hazard assessment is carried out for a proposed nuclear power plant site in PI [14-15]. The purpose of seismic hazard assessment is to generate seismic design basis parameters for the nuclear power plant site [14-15] using probabilistic seismic hazard analysis (PSHA). In this study, the logic tree approach was considered in which all available GMMs [5-13] were considered. However, it was observed that elsewhere GMMs [7-13] are based on seismological parameters of ENA and WNA and two GMMs [5-6] of the Indian region predict very high SAs than expected in the region [14-15]. Hence, in the present study, a new GMM is developed using seismological parameters derived from earthquakes in the Peninsular Indian region.

A typical hard-rock site that has a shear wave velocity (Vs_{30}) of 2.9 km/s (as per soil profile type classification of the national earthquake hazards reduction program (NEHRP)) [14-15] is considered for the present study. The region-specific seismological characteristics, such as the high-frequency decay parameter, anelastic attenuation factor, and stress parameter considered for the present study are obtained from literature on PI earthquakes. The details of various seismological parameters are given in subsequent sections.

2. Stochastic Finite Fault Model for Ground Motion Simulation

The generation of artificial earthquake records is done by using the stochastic finite fault modeling technique [16]. In this technique, the fault plane is modeled as $M \times N$ sub-faults. For ijth sub-fault, the acceleration spectrum $A_{ij}(f)$ is given in Eq. (1).

$$A_{ij}(f)=\frac{CM_{0ij}(2\pi f)^2}{1+(f_{0ij})^2}\times\exp(-\pi f\kappa)\times\exp\left(\frac{-\pi fR_{ij}}{Q\beta}\right)/R_{ij} \quad (1)$$

where M_{0ij}, R_{ij}, and f_{0ij} are seismic moment, hypo-central distance, and corner frequency for ijth sub-fault, kappa (k) is the high-frequency decay parameter and Q is the quality factor.

As shown in Eq. (1), $\exp(-\pi fk)$ models the high-frequency de-amplification from near-surface materials and is characterized by k, known as the high-frequency decay parameter. Another term $\exp\left(\frac{-\pi fR_{ij}}{Q\beta}\right)/R_{ij}$ models the path effect, which includes geometric attenuation ($1/R$) and anelastic attenuation. The anelastic attenuation is inversely related to Q.

Corner frequency, f_{0ij}, is related to the stress drop and is given by:

$$f_{0ij}=4.9E6\times\beta\left(\frac{\Delta\sigma}{M_{0ij}}\right)^{1/3} \quad (2)$$

where $\Delta\sigma$ is the stress drop in bars, M_{0ij} is a seismic moment in dyne/cm and is given by $\log M_0 = 1.5M + 16.1$ and β is shear wave velocity in km/s.

3. Seismological Parameters for Simulation of Artificial Earthquakes

PI has very limited real earthquake data. Seismological parameters such as high-frequency decay parameter, anelastic attenuation factor and stress drop obtained from PI earthquake data are used for the simulation of artificial earthquakes. The details of seismological parameters for the simulation of artificial earthquakes are given below.

3.1. Kappa (k) for Peninsular India (PI)

As discussed, $\exp(-\pi fk)$ models a high-frequency de-amplification from near-surface materials. The k, known as a high-frequency decay parameter, characterizes the high-cut filter. The k is usually obtained from the slope of the Fourier acceleration spectrum at the source or near-field [16]. High-frequency de-amplification effects are represented by two different approaches in the literature.

The first approach was given by Anderson and Hough [17] and also used by Boore [18]. And it can be expressed by:

$$P(f)=\exp(-\pi f\kappa) \quad (3)$$

The second approach given by Hanks [19] is provided by:

$$P(f)=\left[1+\left(\frac{f}{f_m}\right)^8\right]^{-(1/2)} \quad (4)$$

where f_m is a cut-off frequency.

High-frequency de-amplification given by the two approaches will be the same if the following equation is satisfied [19]. It can be expressed by:

$$f_m=\frac{1}{\pi\kappa} \quad (5)$$

The Jabalpur earthquake occurred on May 21st, 1997 [20], and its magnitude (M_w) is 5.8. The SA of this earthquake record is observed to fall beyond a frequency of 32 Hz. Hence, Singh et al. [20] considered cut-off frequency (f_m) as 35 Hz. For the same high-frequency de-amplification, the corresponding value of *k* is about 0.01 using Eq. (5).

On October 16th, 2000 [21], another Jabalpur earthquake occurred with M_w 4.7. In this earthquake record, the SA is observed to fall beyond 17 Hz. For the same high-frequency de-amplification, the corresponding value of *k* is about 0.0187 using Eq. (5). For the Jaitapur site [22], the range of *k* is from 0.01 to 0.016 with a median of 0.013. In the present work, *k* of 0.01, 0.014, and 0.018 are used for artificial earthquake generation.

3.2. Quality factor (Q) for PI

The anelastic attenuation is inversely related to *Q*. The term $\exp\left(\frac{-\pi f R_{ij}}{Q\beta}\right)/R_{ij}$ models the path effect, which includes geometric attenuation (1/R) and anelastic attenuation. Mandal and Rastogi [23] suggested the frequency-dependent quality factor, *Q* as $169f^{0.77}$ for the Koyna region. As the Koyna region has a low *Q*-value, it remains a tectonically active area. *Q*-value obtained from the Indian shield from the 1997 Jabalpur earthquake is $508f^{0.48}$ [20].

The same value is obtained from the 2000 Jabalpur earthquake [21]. For the Jaitapur site [22], the chosen *Q*-values are $84f^{0.65}$, $118f^{0.65}$, and $152f^{0.65}$. It is to be noted that the Q_0-values of the Indian shield region are between 200 and 600 [23]. Hence, the *Q*-factor of $508f^{0.48}$ obtained from the PI earthquake is considered due to proximity and geotechnical similarity.

3.3. Stress parameter (Δσ) for PI

It is defined as the reduction in the value of stress across a fault during a seismic event. Singh et al. [20-21] recommended using 100 and 300 bar as stress drop based on the spectral analysis of the 1997 Jabalpur earthquake [20] and 2000 Jabalpur earthquakes [21]. For the 1967 Koyna earthquake (M_w = 6.3), the predicted ground motion matches the record for a stress drop of 100 bar [20].

The range of 100-300 bar is considered by Raghu Kanth and Iyengar [5] for PI. For the Jaitapur site [22], 140, 170, and 200 bar values are used for the generation of seismic design parameters. Hence, for the simulation of artificial earthquakes, 100 bar, 200 bar, and 300 bar are chosen for stress drop.

3.4. Rupture width and length

Wells and Coppersmith [24] provided the empirical relations for rupture width and rupture length. These relations were obtained from the analysis of various historical earthquakes. The equations used are as follows:

$$\log(A) = a + b \times M \tag{6}$$

$$\log(W) = c + d \times M \tag{7}$$

where *M* is the magnitude, *A* is the rupture area (km^2), *W* is the rupture width (km), *a* = -3.49 and *b* = 0.91 (from 148 earthquake records), and *c* = -1.01 and *d* = 0.32 (from 153 earthquake records) [24].

3.5. Site amplification

Site amplification occurs when seismic waves travel from a rupture source of high shear wave velocity to a surface of a lower value. This is caused by the change in seismic impedance due to the shear wave velocity gradient. In the present study, site amplification for a hard-rock site with a shear wave velocity of 2.9 km/s [25] is used. The site amplification used is given in Table 2.

Table 2 Site amplification with frequency for a hard-rock site with β = 2.9 km/s

Frequency (Hz)	SA
1E-2	1.0
0.1	1.02
0.2	1.03
0.3	1.05
0.5	1.07
0.9	1.09
1.25	1.11
1.8	1.12
3.0	1.13
5.3	1.14
8.0	1.15
14.0	1.15
100.0	1.15

4. Simulation of Artificial Earthquake Records

Parameters for the generation of artificial earthquake records are given in Table 3. Based on the maximum magnitude of the Peninsular Indian region, a magnitude range of 4.5-7.5 is considered. For a generation of design basis ground motion, an area of a 300 km radius around the site is usually considered. Hence, 5-300 km is considered for the epi-central distance range. Depth of focus is varied based on a study for seismic hazard assessment for a typical Peninsular Indian site [14]. The generation is carried out using finite-fault stochastic simulation methodology [16]. A total 12,852 number of artificial earthquake records are generated, for various combinations of parameters given in Table 3. From these 12,852 records, response spectra for 5% damping are obtained as shown in Fig. 1. It can be seen that the PGA (acceleration corresponding to the frequency of 100 Hz) of these 12,852 response spectra has a range of 0.5-1440 gals.

Table 3 Parameters for generation of artificial earthquake records

No.	Parameter	Median value	Range/value
1	k	0.014	0.01-0.018
2	Q	$508f^{0.48}$	
3	Δσ	200	100-300
4	M_w	6.0	4.5, 5.0, 5.5, 6.0, 6.5, 7.0, 7.5
5	Epi-central distance (km)	5, 10, 20,30, 40, 50, 60, 70, 80, 90, 100, 125, 150,175, 200, 250, 300	
6	Depth of focus (km)	d = 5 km ($M_w \leq 5.5$) d = 10 km ($5.5 < M_w < 6.5$) d = 15 km ($6.5 \leq M_w < 7.0$) d = 20 km ($M_w \geq 7.0$)	

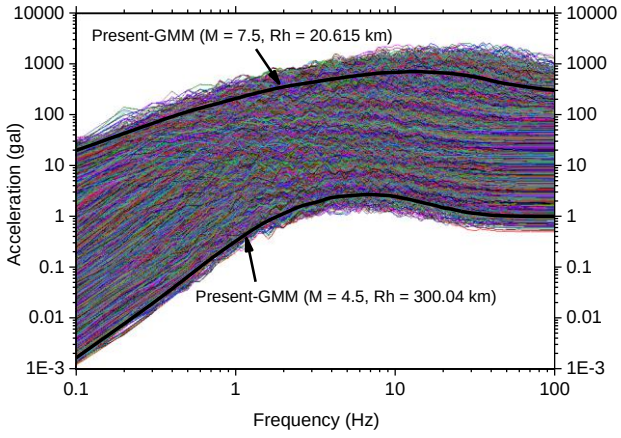

Fig. 1 Response spectra (5% damping) of all artificial records

5. Development of the Present-GMM

The form of the present-GMM is similar to that of an attenuation relation for the intra-plate region [9]. The form of the present-GMM is given in Eq. (8).

$$\log_{10} y_{br} = c_1 + c_2 M + c_3 M^2 + (c_4 + c_5 M) a_2 + (c_6 + c_7 M) a_3 + (c_8 + c_9 M) a_1 + c_{10} R \tag{8}$$

where, $a_1 = \max\left[\log\left(\frac{10}{R}\right), 0\right]$, $a_2 = \max[\log(R), \log 70]$, and $a_3 = \max\left[\log\left(\frac{R}{130}, 0\right)\right]$. It is to be noted that M and R in Eq. (8) correspond to moment magnitude and hypo-central distance respectively. Coefficients of the above frequency-dependent attenuation relation are given in Table 4.

Table 4 Coefficients of present frequency-dependent GMM

Frequency (Hz)	c_1	c_2	c_3	c_4	c_5	c_6	c_7	c_8	c_9	c_{10}	***R*-square**
0.1	-3.5055	0.9682	-0.0814	-5.3108	0.6170	-2.3235	0.1638	4.5892	-1.1207	0.0009	0.972
0.3	-6.8364	2.0656	-0.1658	-4.1702	0.5041	-1.4664	0.0508	6.5860	-1.3171	0.0004	0.968
0.5	-8.6835	2.6196	-0.1999	-3.1674	0.3563	-1.1284	0.0517	9.7760	-1.8752	-0.0001	0.965
0.7	-8.6839	2.6375	-0.2008	-2.6751	0.2952	-0.9429	0.0856	11.2086	-2.2262	-0.0009	0.958
1	-8.1259	2.5228	-0.1914	-2.3588	0.2447	-0.9917	0.0937	8.6866	-1.7789	-0.0010	0.949
1.5	-7.1146	2.2310	-0.1669	-1.9500	0.1858	-0.6576	0.0737	3.8247	-0.8046	-0.0016	0.936
2	-5.7435	1.9008	-0.1437	-2.0452	0.1856	-1.0270	0.0750	-1.3918	0.1522	-0.0012	0.929
2.5	-5.0697	1.7303	-0.1324	-2.0022	0.1826	-0.7988	0.0708	-1.3740	0.1002	-0.0016	0.922
3	-4.5260	1.5970	-0.1226	-2.0131	0.1778	-1.3084	0.0974	-1.0230	0.0340	-0.0012	0.915
3.3	-4.2627	1.5382	-0.1194	-2.0350	0.1829	-1.1641	0.0819	-0.9120	-0.0348	-0.0014	0.915
3.6	-4.0726	1.4774	-0.1141	-1.9689	0.1732	-1.0838	0.0702	-1.3838	0.0529	-0.0015	0.911
4	-3.4808	1.3282	-0.1051	-2.0671	0.1908	-0.8624	0.0627	-3.2702	0.4343	-0.0018	0.909
5	-3.1783	1.2320	-0.0960	-1.9337	0.1687	-1.1496	0.1079	-3.4047	0.5771	-0.0020	0.907
6	-2.6408	1.1218	-0.0905	-2.0650	0.1878	-0.9777	0.0924	-3.2664	0.4486	-0.0023	0.909
7	-2.4356	1.0841	-0.0879	-2.1003	0.1878	-1.0015	0.0761	-2.5430	0.2836	-0.0022	0.908
8	-2.1751	1.0188	-0.0825	-2.0834	0.1809	-1.3408	0.1207	-0.1316	-0.2071	-0.0023	0.908
9	-1.8273	0.9393	-0.0783	-2.1663	0.1938	-1.2833	0.1236	1.5041	-0.5826	-0.0025	0.908
10	-1.6384	0.9151	-0.0787	-2.2552	0.2077	-1.2673	0.1265	2.5458	-0.8271	-0.0027	0.909
12.5	-1.7204	0.9197	-0.0763	-2.1271	0.1850	-1.4519	0.1621	6.2029	-1.4411	-0.0030	0.91
15	-1.4749	0.8703	-0.0747	-2.2080	0.1992	-1.6288	0.2086	8.4817	-1.9191	-0.0033	0.907
18	-1.2144	0.8106	-0.0720	-2.2910	0.2126	-1.5401	0.2107	5.8524	-1.4275	-0.0036	0.909
20	-1.2975	0.8303	-0.0726	-2.2539	0.2044	-1.8178	0.2593	4.0384	-1.0584	-0.0037	0.906
22	-1.3511	0.8235	-0.0702	-2.1772	0.1899	-1.8758	0.2633	4.5023	-1.1098	-0.0036	0.903
25	-1.1998	0.8011	-0.0708	-2.3045	0.2099	-1.8330	0.2738	6.6242	-1.5658	-0.0038	0.901
28	-1.3720	0.8413	-0.0729	-2.2679	0.2029	-1.8068	0.2831	8.2891	-1.8609	-0.0039	0.901
31	-1.2753	0.8333	-0.0740	-2.3614	0.2149	-1.8382	0.2942	8.8317	-1.9756	-0.0039	0.901
34	-1.2287	0.8351	-0.0752	-2.4346	0.2224	-1.8425	0.2877	7.1788	-1.6717	-0.0037	0.901
37	-1.1890	0.8242	-0.0753	-2.4789	0.2313	-1.7675	0.2905	6.3510	-1.5040	-0.0038	0.901
40	-1.1364	0.8124	-0.0758	-2.5290	0.2416	-1.7204	0.2976	6.2781	-1.4935	-0.0039	0.901
45	-1.1441	0.8153	-0.0773	-2.5934	0.2530	-1.6469	0.2851	5.5864	-1.3394	-0.0038	0.903
50	-1.2010	0.8210	-0.0771	-2.5804	0.2491	-1.7180	0.2882	4.7007	-1.1373	-0.0036	0.911
70	-1.4423	0.8682	-0.0805	-2.6012	0.2505	-1.7797	0.2676	4.6914	-1.1002	-0.0030	0.903
100	-1.6305	0.8872	-0.0813	-2.5688	0.2495	-1.7994	0.2489	3.7024	-0.8913	-0.0027	0.901

The standard deviation $\log_{10} y_{br}$ at all frequencies is 0.25. The *R*-square value for each frequency is provided in Table 4. It can be seen that *R*-square values are more than 0.9 for all frequencies, which indicates that a good fit is chosen for regression. It is a standard practice to plot the regression residuals to verify whether the correct fit is chosen to reproduce the simulations. If there is no significant residual trend with distance or magnitude, it can be inferred that a good fit is chosen for regression. Regression residuals versus distance are plotted for M_w 5.0 as shown in Fig. 2. Fig. 3 shows the plot of regression residuals with a distance of M_w 6.0. The plot of regression residuals for M_w 7.0 is shown in Fig. 4. It can be seen that no considerable residual trend is observed from these figures.

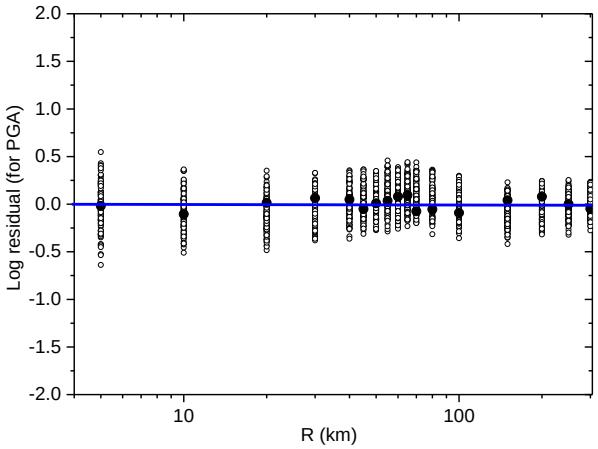

Fig. 2 Plot of residuals for M_w 5.0

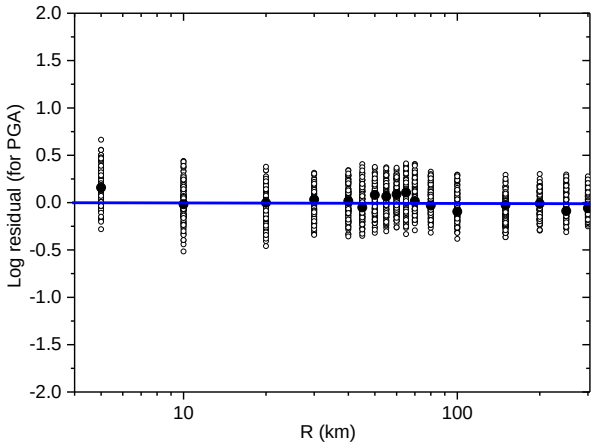

Fig. 3 Plot of residuals for M_w 6.0

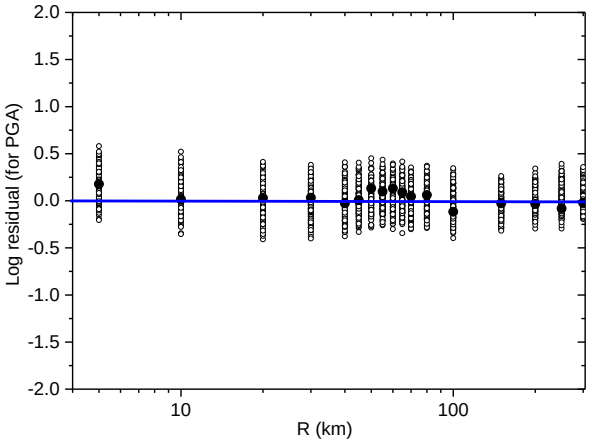

Fig. 4 Plot of residuals for M_w 7.0

The present-GMM is valid for a magnitude range of 4.5-7.5 and an epi-central distance range of 5-300 km. The lowest possible spectral acceleration (SA) by present-GMM corresponds to a magnitude of 4.5 and an epi-central distance of 300 km. As the depth of focus considered for a magnitude of 4.5 is 5 km, the corresponding hypo-central distance is 300.04 km. The highest possible SA by present-GMM corresponds to a magnitude of 7.5 and an epi-central distance of 5 km. As the depth of focus considered for a magnitude of 7.5 is 20 km, the corresponding hypo-central distance is 20.615 km. The lowest and highest possible SAs by present-GMM (Eq. (8)) are shown in Fig. 1. It can be seen that the PGA (acceleration corresponding to the frequency of 100 Hz) predicted by GMM has a range of 1-300 gals, which is lying in the range of individual records.

6. Comparison of Predictions of Present-GMM with Other Intra-Plate Ground Motion Relations for Hard-Rock

The comparison of predictions of present-GMM, with other intra-plate ground motion relations for hard-rock for M_w 5.0 is shown in Fig. 5. The prediction of various GMMs for PGA corresponding to various distances (hypo-central distance) and

M_w 5.0 is shown in Fig. 5(a). It can be seen that NDMA-2010 and RI-2007 predict much higher PGA values compared to other GMMs. Peza-2011 predicts higher PGA values for distances up to 15 km. The present-GMM's predictions are lying in the band of predictions by other GMMs. Various GMM predictions of 5% damped response spectra for M_w 5.0 and R_h = 50 km are given in Fig. 5(b).

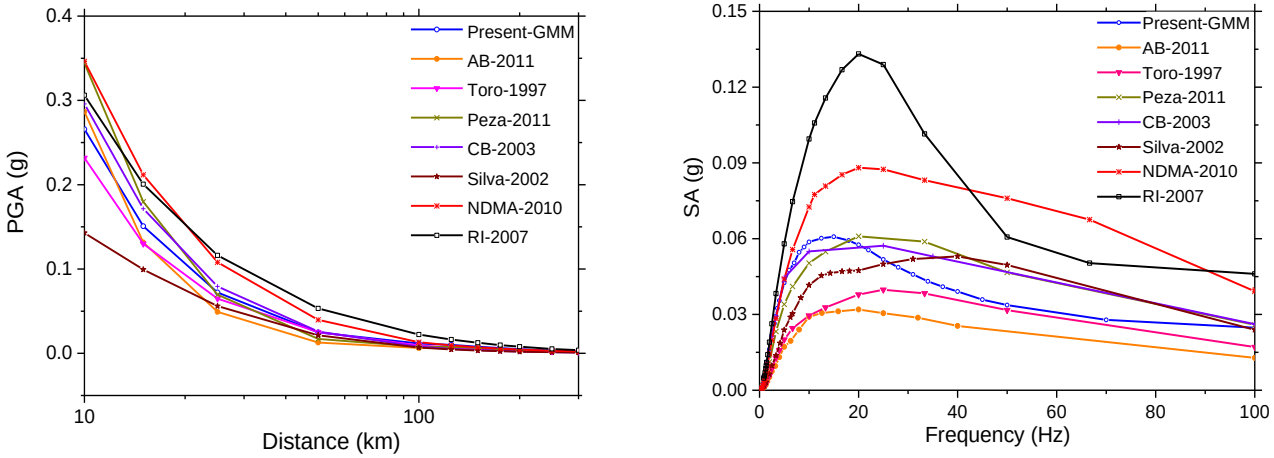

(a) PGA of M_w 5.0 (b) 5% damped response spectra for M_w 5.0 and R_h = 50 km

Fig. 5 Comparison of other hard-rock ground motion relations with the present-GMM for M_w 5.0

It can be seen that NDMA-2010 and RI-2007 predict higher SAs compared to other GMMs. The response spectrum predicted by the present-GMM lies in the band of predictions by other GMMs. Also, the SAs predicted by the present-GMM are in the range of predictions of other international GMMs. However, the frequency band is relatively lower than those of other GMMs. The comparison for M_w 6.0 is shown in Fig. 6. The PGA comparison for various distances is shown in Fig. 6(a). Response spectral comparison for M_w 6.0 and R_h = 50 km is given in Fig. 6(b). It can be seen that NDMA-2010 and RI-2007 have given higher predicted PGA and SA values in comparison with other GMMs. It can be observed that predictions by present-GMM are lying in the range of predictions of other GMMs.

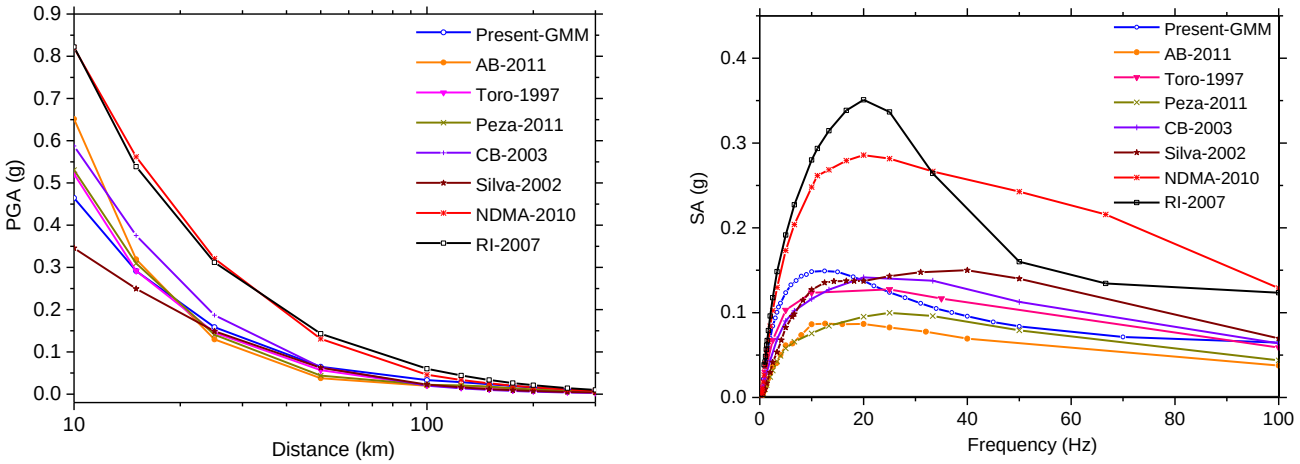

(a) PGA of M_w 6.0 (b) 5% damped response spectra for M_w 6.0 and R_h = 50 km

Fig. 6 Comparison of other hard-rock ground motion relations with the present-GMM for M_w 6.0

The comparison for M_w 7.0 is shown in Fig. 7. The PGA comparison for various distances is shown in Fig. 7(a). Response spectral comparison for M_w 7.0 and R_h = 50 km is given in Fig. 7(b). It can be seen that NDMA-2010 and RI-2007 have given higher predicted PGA and SA values when compared with other GMMs. However, for short distances (up to 30 km), NDMA-2010 predictions are relatively lower than RI-2007. It can be noticed that predictions by the present-GMM are lying in the range of predictions of other intra-plate ground motion relations for hard-rock.

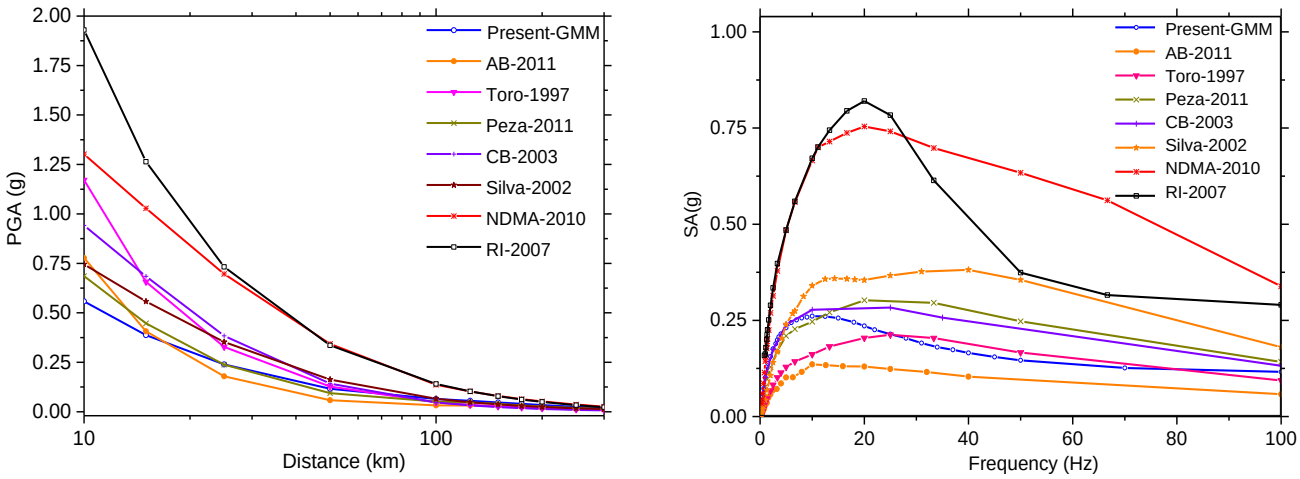

(a) PGA of M_w 7.0 (b) 5% damped response spectra for M_w 7.0 and R_h = 50 km

Fig. 7 Comparison of other hard-rock ground motion relations with the present-GMM for M_w 7.0

7. Comparison of Present-GMM Predictions with Strong Ground Motion Data of Koyna Earthquake

Strong ground motion availability for the Peninsular Indian region is scarce. The Koyna earthquake is one of the few earthquakes that occurred in the Peninsular Indian region. An M_w 6.5 earthquake struck on December 10th, 1967 in Koyna [26]. This is one of the major seismic events for which instrumental strong ground motion data is available. The horizontal acceleration record of this earthquake at an epi-central distance of 12.74 km is shown in Fig. 8. Corresponding response spectrum along with estimated spectra from various GMMs are shown in Fig. 9. A comparison of the frequency content of the Koyna earthquake with other GMMs is shown in Fig. 10.

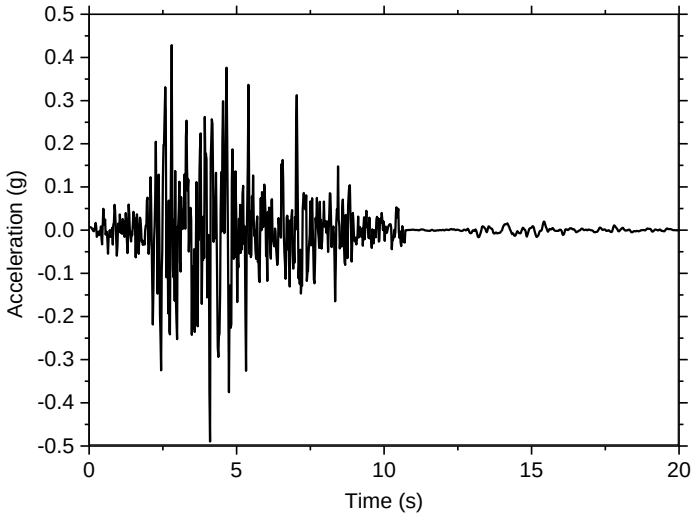

Fig. 8 Accelerogram of Koyna earthquake

It is observed that the response spectrum predicted by the present-GMM compares well with the actual earthquake record. From the frequency content shown in Fig. 9, it is observed that response spectra of other internationally available GMMs contain relatively higher frequency content as compared to the present-GMM and Koyna earthquake records. This can be attributed to the high-cut filter term in the ground motion simulations. It may also be due to the relatively smaller value of k = 0.005 for ENA [9] as compared to the relatively higher value of k = 0.01-0.018 for PI.

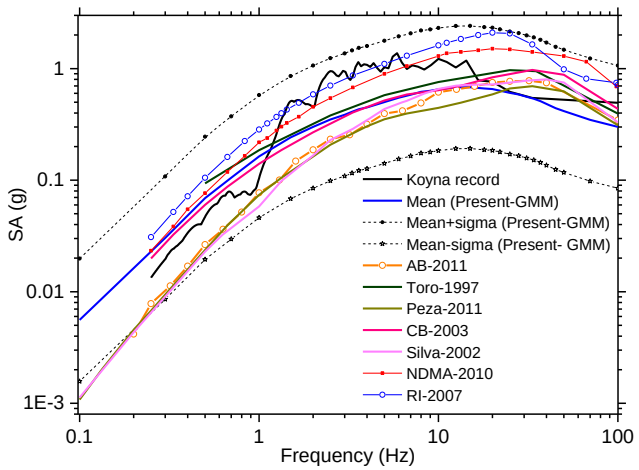

Fig. 9 Comparison of response spectrum of Koyna earthquake with other hard-rock ground motion relations and present-GMM

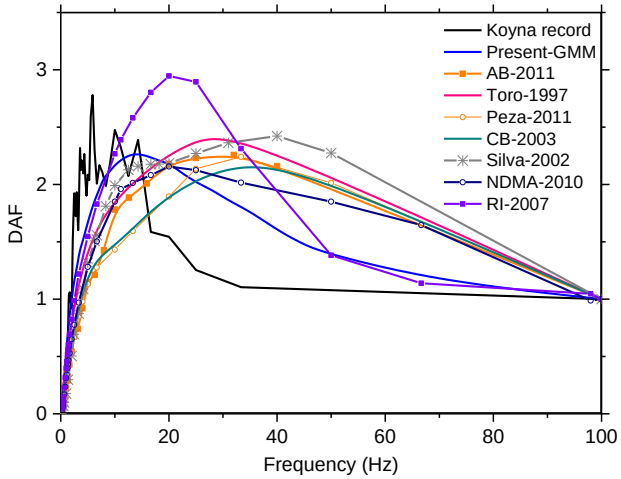

Fig. 10 Comparison of the frequency content of the Koyna earthquake with otherhard-rock ground motion relations and present-GMM

8. Results and Discussion

Seismological parameters derived from earthquakes in the Peninsular Indian region are used to generate 12,852 artificial earthquake records. Constants of the present-GMM are obtained by regression of response spectra of all these records. The present-GMM is applicable for M_w 4.5-7.5 and an epi-central distance range of 5-300 km.

The predictions of present-GMM are compared with other intra-plate ground motion relations for hard-rock. It is observed that two other earlier GMMs of PI have predicted higher PGA and SA values when compared with other GMMs. It is also observed that predictions by present-GMM are lying in the range of predictions of other GMMs.

The SAs predicted by the present-GMM compare well with that of the actual Koyna earthquake. SAs of other internationally available GMMs contain relatively higher frequency content as compared to the present-GMM and the Koyna earthquake record. This can be attributed to the relatively higher value of the spectral decay parameter for PI when compared with that of ENA. The present-GMM can be further improved by refining the seismological parameters using future earthquake records if any.

9. Conclusions

The present-GMM based on the regression of simulated accelerograms was generated for a PI hard-rock site. The following conclusions are drawn from the present study:

(1) As artificial earthquakes are simulated using seismological parameters from actual earthquakes of PI, the present-GMM is applicable.

(2) As R-square values are more than 0.9 for all frequencies, it can be confirmed that a good fit is chosen for regression.

(3) Present-GMM is compared with other intra-plate ground motion relations for hard-rock. The comparison shows that the present-GMM's predictions are well within the band of predictions by other intra-plate ground motion relations.

(4) Finally, the present-GMM is validated with the record of the Koyna earthquake of PI. It is observed that the present-GMM's predictions are closer to the actual earthquake record of the Peninsular Indian region as compared to other GMMs. Therefore, it can be concluded that the present-GMM can be used to evaluate ground motion parameters for the Peninsular Indian hard-rock site.

Conflicts of Interest

The authors declare no conflict of interest.

References

[1] S. K. Nath and K. K. S. Thingbaijam, "Peak Ground Motion Predictions in India: An Appraisal for Rock Sites," Journal of Seismology, vol. 15, no. 2, pp. 295-315, April 2011.

[2] M. L. Sharma, J. Douglas, H. Bungum, and J. Kotadia, "Ground-Motion Prediction Equations Based on Data from the Himalayan and Zagros Regions," Journal of Earthquake Engineering, vol. 13, no. 8, pp. 1191-1210, 2009.

[3] R. Ramkrishnan, K. Sreevalsa, and T. G. Sitharam, "Development of New Ground Motion Prediction Equation for the North and Central Himalayas Using Recorded Strong Motion Data," Journal of Earthquake Engineering, vol. 25, no. 10, pp. 1903-1926, 2021.

[4] K. Bajaj and P. Anbazhagan, "Determination of GMPE Functional Form for an Active Region with Limited Strong Motion Data: Application to the Himalayan Region," Journal of Seismology, vol. 22, no. 1, pp. 161-185, January 2018.

[5] S. T. G. Raghu Kanth and R. N. Iyengar, "Estimation of Seismic Spectral Acceleration in Peninsular India," Journal of Earth System Science, vol. 116, no. 3, pp. 199-214, June 2007.

[6] Working Committee of Experts (WCE), "Development of Probabilistic Seismic Hazard Map of India," NDMA (National Disaster Management Authority), Government of India, Technical Report, 2010.

[7] E. Schweig, J. Gomberg, M. D. Petersen, M. Ellis, P. Bodin, L. Mayrose, et al., "The Mw 7.7 Bhuj Earthquake: Global Lessons for Earthquake Hazard in Intra-Plate Regions," Journal of the Geological Society of India, vol. 61, no. 3, pp. 277-282, 2003.

[8] G. M. Atkinson and D. M. Boore, "Modifications to Existing Ground-Motion Prediction Equations in Light of New Data," Bulletin of the Seismological Society of America, vol. 101, no. 3, pp. 1121-1135, June 2011.

[9] G. M. Atkinson and D. M. Boore, "Earthquake Ground-Motion Prediction Equations for Eastern North America," Bulletin of the Seismological Society of America, vol. 96, no. 6, pp. 2181-2205, December 2006.

[10] G. R. Toro, N. A. Abrahamson, and J. F. Schneider, "Model of Strong Ground Motions from Earthquakes in Central and Eastern North America: Best Estimates and Uncertainties," Seismological Research Letters, vol. 68, no. 1, pp. 41-57, January/February 1997.

[11] S. Pezeshk, A. Zandieh, and B. Tavakoli, "Hybrid Empirical Ground-Motion Prediction Equations for Eastern North America Using NGA Models and Updated Seismological Parameters," Bulletin of the Seismological Society of America, vol. 101, no. 4, pp. 1859-1870, August 2011.

[12] K. W. Campbell, "Prediction of Strong Ground Motion Using the Hybrid Empirical Method and Its Use in the Development of Ground-Motion (Attenuation) Relations in Eastern North America," Bulletin of the Seismological Society of America, vol. 93, no. 3, pp. 1012-1033, June 2003.

[13] W. Silva, N. Gregor, and R. Darragh, "Development of Regional Hard Rock Attenuation Relations for Central and Eastern North America," Pacific Engineering and Analysis, https://www.nrc.gov/docs/ML0423/ML042310569.pdf, November 2002.

[14] A. Ravi Kiran, M. H. Prasad, M. K. Agrawal, G. Vinod, and G. R. Reddy, "Seismic Hazard Assessment and Uniform Hazard Response Spectrum (UHRS) Generation for Tarapur Site," Ref. AHWR/DBGM/01900/R0/190513, Technical report, 2019.

[15] A. Ravi Kiran, S. Bandopadhyay, M. K. Agrawal, G. R. Reddy, and R. K. Singh, "Generation of Uniform Hazard Response Spectrum for a Peninsular Indian Site," International Journal of Earth Sciences and Engineering, vol. 8, no. 2, pp. 332-335, April 2015.

[16] D. Motazedian and G. M. Atkinson, "Stochastic Finite-Fault Modeling Based on a Dynamic Corner Frequency," Bulletin of the Seismological Society of America, vol. 95, no. 3, pp. 995-1010, June 2005.

[17] J. G. Anderson and S. E. Hough, "A Model for the Shape of the Fourier Amplitude Spectrum of Acceleration at High Frequencies," Bulletin of the Seismological Society of America, vol. 74, no. 5, pp. 1969-1993, October 1984.

[18] D. M. Boore, "Short-Period P- and S-Wave Radiation from Large Earthquakes: Implications for Spectral Scaling Relations," Bulletin of the Seismological Society of America, vol. 76, no. 1, pp. 43-64, February 1986.

[19] T. C. Hanks, "fmax" Bulletin of the Seismological Society of America, vol. 72, no. 6A, pp. 1867-1879, December 1982.

[20] S. K. Singh, M. Ordaz, R. S. Dattatrayam, and H. K. Gupta, "A Spectral Analysis of the 21 May 1997, Jabalpur, India, Earthquake (Mw = 5.8) and Estimation of Ground Motion from Future Earthquakes in the Indian Shield Region," Bulletin of the Seismological Society of America, vol. 89, no. 6, pp. 1620-1630, December 1999.

[21] S. K. Singh, S. D. Pimprikar, B. K. Bansal, J. F. Pacheco, R. S. Dattatrayam, and G. Suresh, "An Analysis of the Mw 4.7 Jabalpur, India, Earthquake of 16 October 2000: Toward Ground-Motion Estimation in the Region from Future Events," Bulletin of the Seismological Society of America, vol. 97, no. 5, pp. 1475-1485, October 2007.

[22] B. K. Rastogi and A. G. Chhatre, "Seismotectonic Investigations for Siting of Nuclear Power Plants, Assessment of Design Basis Ground Motion and Tsunami Hazard," Journal of Indian Society of Earthquake Science, vol. 1, pp. 93-109, December 2014.

[23] P. Mandal and B. K. Rastogi, "A Frequency-Dependent Relation of Coda Qc for Koyna-Warna Region, India," Pure and Applied Geophysics, vol. 153, no. 1 pp. 163-177, November 1998.

[24] D. L. Wells and K. J. Coppersmith, "New Empirical Relationships among Magnitude, Rupture Length, Rupture Width, Rupture Area, and Surface Displacement," Bulletin of the Seismological Society of America, vol. 84, no. 4, pp. 974-1002, August 1994.

[25] D. M. Boore and W. B. Joyner, "Site Amplifications for Generic Rock Sites," Bulletin of the Seismological Society of America, vol. 87, no. 2, pp. 327-341, April 1997.

[26] A. N. Tandon and H. M. Chaudhury, "Koyna Earthquake of December 1967," India Meteorological Department, Scientific Report, no. 59, 1968.